Bulletin of the Seismological Society of America, Vol. 99, No. 5, pp. 2979–2991, October 2009, doi: 10.1785/0120080272

Importance of Mapping Design Earthquakes: Insights for the Southern Apennines, Italy

by Vincenzo Convertito, Iunio Iervolino, and André Herrero

Abstract Probabilistic seismic hazard analysis is currently the soundest basis for the rational evaluation of ground-motion hazard for site-specific engineering design and assessment purposes. An increasing number of building codes worldwide acknowledge the uniform hazard spectra as the reference to determine design actions on structures and to select input ground motions for seismic structural analysis. This is the case, for example, in Italy where the new seismic code also requires the seismic input for nonlinear dynamic analysis to be selected on the basis of dominating events, for example, identified via disaggregation of seismic hazard. In the present study, the design earthquakes expressed in terms of representative magnitude (M), distance (R), and ε were investigated for a wide region in the southern Apennines, Italy. To this aim, the hazards corresponding to peak ground acceleration and spectral acceleration at 1 sec with a return period of 475 yr were disaggregated. For each of the disaggregation variables the shape of the joint and marginal probability density functions were studied. The first two modes expressed by M, R, and ε were extracted and mapped for the study area. The results shown provide additional information, in terms of source and ground-motion parameters, to be used along with the standard hazard maps to better select the design earthquakes. The analyses also allow us to assess how various frequency ranges of the design spectrum are differently contributed by seismic sources in the study area.

Introduction

From an engineering point of view, the most accurate analysis to assess the safety level of civil and/or strategic structures, such as nuclear power plants, hospitals, bridges, or lifelines in an earthquake-prone zone, implies nonlinear dynamic analysis. It allows accounting for several characteristics of ground shaking, such as peculiar spectral shape, cumulative damage potential such as duration, nonstationarity, and special effects such as directivity-related velocity pulses (see, e.g., Iervolino and Cornell, 2008). As a consequence, it requires detailed modeling of the structure and proper selection of the seismic ground-motion input. The latter typically consists of a suite of time series representative of ground shaking that the structure must withstand during its lifetime, based on the hazard at the site where it is located. The selection of recorded waveforms from a given database, or their simulation through *ad hoc* techniques, may require that one or more earthquakes, defined as the design earthquakes, are prudently identified (Iervolino and Cornell, 2005). In fact, when selection of recorded waveforms for seismic design of structures is concerned, the current state of best engineering practice (e.g., U.S. Nuclear Regulatory Commission, 2001) is based on the uniform hazard spectrum (UHS), which is an elastic response spectrum (commonly, 5% critically damped) derived from the analysis of the probabilistic seismic hazard at the site. The UHS is defined with the purpose that all its spectral ordinates have the same probability of exceedance in a time interval depending on the limit state of interest[1]. Once the UHS has been defined, the waveforms' selection proceeds with the disaggregation of seismic hazard (e.g., McGuire, 1995; Bazzurro and Cornell, 1999) by M (magnitude), R (distance), and ε (epsilon, defined as the number of standard deviations by which the logarithmic ground motion departs from the median predicted by an appropriate attenuation relationship) for the level of spectral acceleration given by the UHS at the first mode period of the structure[2].

[1]Although the use of UHS was only recently acknowledged by engineering practice and/or codes for design and assessment purposes (e.g., in Italy), the concept of UHS is not new, and some studies have already investigated the shortcomings of this kind of representation of ground motion and propose more sound alternatives (see, e.g., Baker and Cornell, 2006).

[2]Epsilon may be important because in the case of time histories to be used as the input for structural dynamic analysis, high epsilon values are associated with peaks in the response spectrum of the record. During shaking, the effective period of the structure lengthens, lowering the peak toward a less energetic portion of the frequency content; therefore, ground-motion

Disaggregation is based on the assessment of the relative contributions of the elements used to compute seismic hazard, for example, seismogenic zones, recurrence relationships, and as recently investigated, focal mechanisms (Convertito and Herrero, 2004). In other words, because probabilistic seismic hazard analysis (PSHA) implies vast homogenization of the various contributing earthquake sources to site hazard, disaggregation allows the identification of the earthquakes that dominate the hazard as a function of the structural oscillation period, location, and return period. Those contributions are typically expressed in terms of probability density functions (PDFs) of M, R, and ε conditional to the exceedance of the level of spectral acceleration, Sa(T), for which the hazard is disaggregated. The analysis of these PDFs allows the definition of the design earthquakes identifying the values of the variables giving the largest contribution to the hazard or considered representative in some other statistical sense.

Given the dominant M, R, and ε sets, along with other earthquake-specific factors, such as directivity, faulting style, and duration, site-specific realistic time histories can be recommended for engineering analyses. In fact, after the so-defined design earthquakes are identified, a database is accessed, and a number of time histories is selected to match, within tolerable limits, the values of these parameters believed to be important for a correct estimation of the structural response. (Note that this is an approximation; in principle one should account for the whole $M - R - \varepsilon$ distribution in record selection.)

Finally, the selected time histories are scaled to match precisely the UHS level at the first period (T) of the structure. Time histories obtained in this way are used as the input for a set of nonlinear dynamic analyses to evaluate the behavior of the structure in the case of the ground motion represented by the UHS (Cornell, 2004, 2005).

Generally, prescriptions for time-histories selection in building codes (e.g., EN 1998-1, 2004) only approximate the approach discussed previously (see Iervolino *et al.*, 2008, 2009). In fact, the code-based spectra may be very weakly related to the hazard and, therefore, may be quite different from the UHSs. In these cases disaggregation may still be useful to identify the controlling earthquake sources, but to relate the design spectra to the hazard requires the PSHA to be available for any site in the region where the code applies. This is not the case for many countries where engineers are seldom able to easily run or obtain hazard analyses for the site of interest. A fortunate case in this respect is the United States, where hazard data may be downloaded by the U.S. Geological Survey (USGS) Web site. Italy also now has a similar service because of the excellent work of the Istituto Nazionale di Geofisica e Vulcanologia (INGV) carried out in the framework of a specific project (see the Data and Resources section) commissioned between 2004 and 2006 by the Italian Civil Protection-Dipartimento della Protezione Civile (DPC). The results of the project include hazard curves on rock based on 9 return periods for 11 oscillation periods of engineering interest and disaggregation of peak ground acceleration (PGA) hazard for the whole Italian territory (Meletti and Montaldo, 2007; Montaldo and Meletti, 2007). This study has been acknowledged by the new Italian seismic code (CS.LL.PP., 2008) that now allows us to design considering response spectra derived from seismic hazard (technically coincident with the UHSs) and, in principle, to select time histories with respect to the characteristics of the dominating earthquakes.

The study herein presented, based on similar premises of what was proposed by Cramer and Petersen (1996) for southern California and Harmsen and Frankel (2001) for the United States, investigates the implications of mapping the design earthquakes for spectral accelerations corresponding to different spectral frequency ranges via an application to the Campania–Lucania region in southern Apennines, Italy. In fact, the data made publicly available for Italy by INGV include disaggregation for PGA only (Spallarossa and Barani, 2007); however, short and long period ranges of the UHS may be affected by different seismic sources in terms of magnitude and distance (Reiter, 1990). This is important because design of moderate-to-long period structures has to consider dominant events that may be not well represented by the results of PGA hazard disaggregation.

For the area considered, maps of the first two modal magnitude, distance, and epsilon sets were computed from disaggregation of seismic hazard on rock sites specifically calculated for two spectral ordinates, PGA and Sa($T = 1$ sec). The selected hazard level corresponds to 10% exceedance probability in 50 yr, which is a reference return period for the life-safety limit state of ordinary constructions. These maps may be tools to define the dominating earthquakes for each site (Bommer, 2004) and to assess how different frequencies of the design spectrum are differently contributed by seismogenic sources in the area.

Methodology

The result of PSHA, for a selected site, is a hazard curve that represents the probability of exceedance of a ground-motion parameter A in a time interval of interest (e.g., the design life of a structure). The construction of the hazard curve requires the computation of the hazard integral (Cornell, 1968; Bazzurro and Cornell, 1999) that, for the ith selected seismogenic zone and a range of possible magnitudes and distances, provides the mean annual rate of exceedance as in equation (1),

records with high epsilon values may be associated with a more benign structural response. The opposite happens to negative epsilon records. Therefore, when selecting waveforms for structural analysis, one should consider choosing them among those having the right epsilon, that is, the one dominating the hazard at the site, for an unbiased estimation of structural response (Cornell, 2004; Baker and Cornell, 2006).

$$E_i(A > A_0) = \alpha_i \int_M \int_R \int_\varepsilon I[A > A_0|m, r, \varepsilon] f(m) f(r) f(\varepsilon)\, dm dr d\varepsilon, \quad (1)$$

where I is an indicator function that equals 1 if A is larger than A_0 for a given distance r, ranging between $R_{\min}$ and $R_{\max}$, a given magnitude m, ranging between $M_{\min}$ and $M_{\max}$ and a given ε, which represents the residual variability of the A parameter with respect to the selected attenuation relationship. The PDFs of M, $f(m)$, and R, $f(r)$, depend, respectively, upon the adopted earthquake recurrence model (e.g., Gutenberg and Richter, 1944) and upon the source geometry that can be a point, a line, a plane or an areal source zone. Finally, α_i for each zone, represents the mean annual rate of occurrence of the earthquakes within the source.

Assuming a Poissonian (homogenous) recurrence model, equation (1) allows the computation of the probability of exceedance P in a time interval t as in equation (2), where the sum is over all the sources contributing to the hazard,

$$P(A > A_0, t) = 1 - e^{-\sum_{i=1}^{N} E_i(A>A_0)\cdot t}. \quad (2)$$

PSHA, for its integral nature, combines the contribution to the hazard from all N considered sources. On the other hand, for engineering purposes it may be important to identify the most threatening earthquakes for the site of interest. The procedure that allows the decomposition of each point on the hazard curve, in terms of M and R, from each different source is disaggregation. In the last decade, it has become common practice to also look at the disaggregation of seismic hazard in terms of ε. Given magnitude and distance, ε represents, via its associated PDF, $f(\varepsilon)$, the variability of the ground-motion parameter for which the hazard is estimated. As briefly mentioned previously, disaggregation in terms of ε may be useful to choose records for nonlinear dynamic analysis having the correct spectral shape at a period relevant for the dynamic behavior of the structure.

From an analytical point of view, the disaggregation's result is the joint PDF in equation (3),

$$f(m, r, \varepsilon|A > A_0) = \frac{\sum_{i=1}^{N} \alpha_i I[A > A_0|m, r, \varepsilon] f(m) f(r) f(\varepsilon)}{\sum_{i=1}^{N} E_i(A > A_0)}, \quad (3)$$

which is the distribution of magnitude, distance, and ε conditional on the exceedance of the hazard level being disaggregated. In other words, given the exceedance of the A_0 ground-motion value, disaggregation provides how likely it is caused by each specific M, R, ε set (McGuire, 1995).

From the PDF in equation (3) marginal PDFs may be obtained. They are univariate distributions of the disaggregation variables. The marginal PDF of a variable is obtained from the joint PDF saturating the other variables, that is, adding up all their contributions (Benjamin and Cornell, 1970). This gives the contribution to hazard of each variable alone. Marginal PDFs for M, R, and ε may be computed with equations from (4) to (6),

$$f(m|A > A_0) = \int_R \int_\varepsilon f(m, r, \varepsilon|A > A_0)\, dr d\varepsilon, \quad (4)$$

$$f(r|A > A_0) = \int_M \int_\varepsilon f(m, r, \varepsilon|A > A_0)\, dm d\varepsilon, \quad (5)$$

$$f(\varepsilon|A > A_0) = \int_M \int_R f(m, r, \varepsilon|A > A_0)\, dm dr. \quad (6)$$

In the case one wants or is allowed by the seismic code to use disaggregation of seismic hazard to identify the design earthquakes for the site of interest, semiarbitrary approaches based on these PDFs are usually adopted. For example, representative values of the distributions (e.g., median, modal, or the mean values of M, R, and ε) may be considered if a single design earthquake is sought.

The first step in the analyses of the present study consisted of the computation of the hazard maps for the region shown in Figure 1, in terms of PGA and Sa($T = 1$ sec). The choice of these two spectral ordinates is to represent the high and moderate-to-low frequency branches of the response spectrum, respectively. This is important because, although this has been known for some time, often both seismologists and engineers focus on hazard in terms of PGA only; on the other hand, seismic structural response is more sensitive to the spectral ordinates corresponding to lower frequencies. Therefore, the hazard should be better expressed in terms of spectral ordinates close to the fundamental period of the structure for which the seismic design or assessment is carried out. In fact, because disaggregation results, apart from the return period, also depend on such ordinates, a comparison of the design earthquakes resulting from disaggregation of PGA and other spectral ordinates is worthwhile. In the United States, for example, the disaggregation is often done at 0.2 sec, while herein Sa($T = 1$ sec) hazard is considered as it could be of interest for most of the common structures.

Probabilistic Seismic Hazard for Southern Apennines

The southern Apennines are an active seismogenic belt consisting of different faults which were the site of historical earthquakes (e.g., in 1456, 1694, 1851, 1857, and 1930) and recent moderate seismicity (e.g., the 5 May 1990 Potenza M_w 5.8 earthquake). The last destructive earthquake occurring in the area of interest was the complex Irpinia earthquake (23 November 1980, M_w 6.9) that caused about 3000 deaths and enormous damage (Westaway and Jackson, 1987). Most of the instrumentally recorded earthquakes have occurred in a narrow band along the Apennine chain (corresponding to

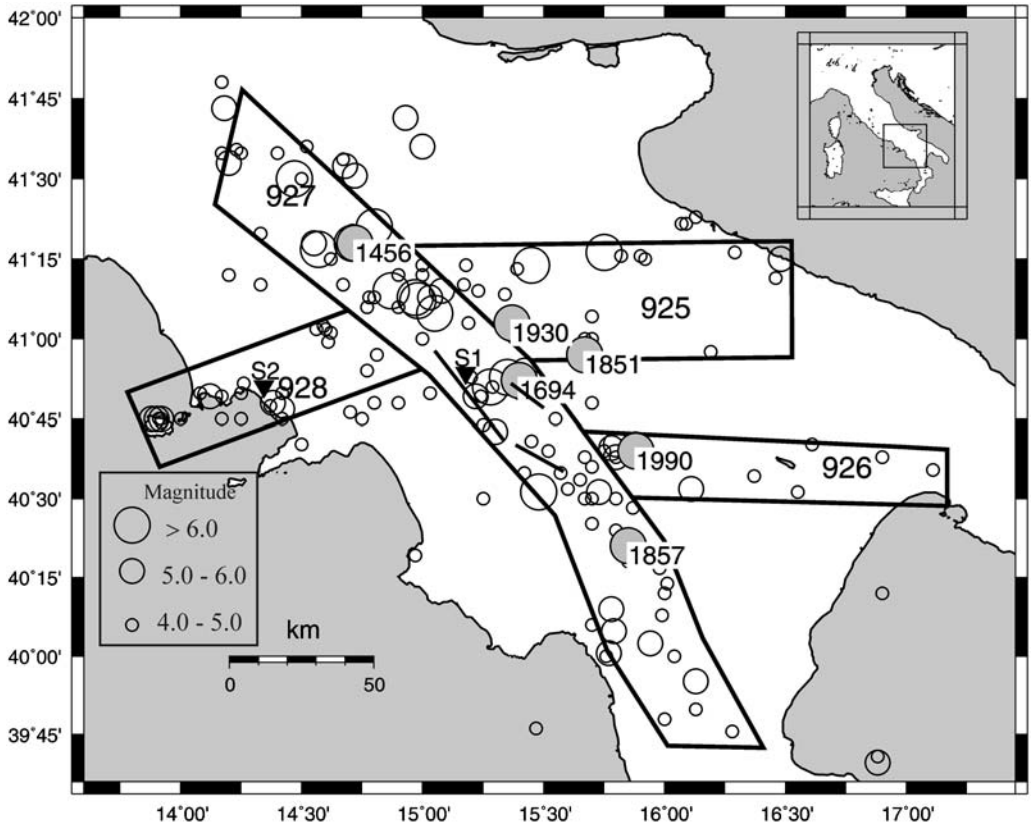

Figure 1. Seismic source zone configuration used to compute the hazard and design earthquakes maps. Location of the sites S1 and S2 used in the analysis is identified by black triangles. Circles, whose width is proportional to magnitude, represent the location of the earthquakes ($M > 4.0$) retrieved from the CPTI04 catalog (Gruppo di lavoro Catalogo Parametrico dei Terremoti Italiani [CPTI], 2004). Labels report the dates of some historical earthquakes. Black lines represent the surface projection of the three fault segments which ruptured during the 23 November 1980 Irpinia earthquake.

zone 927 in Fig. 1) in the top 20 km of the crust and reveals a prevailing extensional regime (Montone *et al.*, 2004) as indicated by normal faulting mechanisms (Valensise *et al.*, 2003; Meletti *et al.*, 2008). Furthermore, a recent study by Cinti *et al.* (2004) has shown that the southern Apennines region has a significant probability of occurrence for $M \geq 5.5$ earthquakes in the next 10 yr. These considerations render the area a good candidate for the application of hazard and disaggregation analysis discussed previously.

Concerning the hazard elements, the modeling of the seismogenic zones in the southern Apennines region is that of the Italian zonation (ZS9) also adopted by the INGV (Meletti *et al.*, 2008), along with the activity rates, b-values, and minimum and maximum magnitudes that are listed in Table 1. Figure 1 shows the location and the dates of the historical earthquakes cited previously; moreover, events with magnitude larger than M 4.0, contained in the CPTI04 catalog (see the Data and Resources section) provided by the CPTI (2004) and used by INGV to compute the national hazard maps, are also shown. Finally, the same figure reports the three fault segments on which the 23 November 1980 M_w 6.9 Irpinia earthquake originated. The activity rates and the values selected for the analyses performed in this work are based on the historical catalog adjusted for completeness. The historical catalog also contains the main instrumental recorded earthquakes that occurred in the study area. The selected attenuation relationship considered is that of Sabetta and Pugliese (1996), which is derived from Italian strong-motion data.

The hazard maps have been computed for PGA and Sa($T = 1$ sec) for the return period $T_R = 475$ yr. To this aim, the numerical computation of equation (1) was carried out using relatively small increments: 1.0 km for distance, 0.05 for magnitude, and 0.2 for ε. These steps reduce the problems of numerical interpolation commonly used to produce the hazard maps and, from a disaggregation point of view, allow to limit the issues related to the appropriate selection of the bins used to collect the contributions of the hazard variables. In fact, the identification of the modes of

Table 1
Parameters of the Selected Seismogenic Zones Shown in Figure 1

Zone	α (events/yr)	b	M_{min}	M_{max}
925	0.17	−0.75	4.0	6.83
926	0.09	−1.38	4.0	6.14
927	0.69	−0.72	4.0	7.06
928	0.21	−0.66	4.0	5.91

the PDFs may depend on the size of the M, R, and ε bins used for disaggregation.

Panel (a) of Figure 2 shows the hazard map for PGA, and panel (b) shows the map for Sa($T = 1$ sec); both are expressed in units of g. Because of the values of the input parameters and its areal extension, the most hazardous seismic zone is the zone 927.

To better understand the results for the region, the hazard computed for two specific sites is discussed. The selected sites are Sant'Angelo dei Lombardi, indicated as S1 (latitude: 40.8931° N, longitude: 15.1784° E), and Ponticelli (Naples), indicated as S2 (latitude: 40.8516° N, longitude: 14.3446° E). The two sites, shown in Figure 1 (black triangles), have been selected based on the fact that site S1 is located in the epicentral area of the 23 November 1980 Irpinia earthquake, and site S2 is the construction site of one of the largest seismically isolated structures in Europe (Di Sarno *et al.*, 2006).

The site-specific analysis will be used to show how the hazard at the two sites can be affected by the parameterization of the selected seismogenic sources. The UHSs are also computed and compared to that provided by INGV, which may be considered as a benchmark. The comparison is only qualitative because INGV used a more sophisticated approach, based on logic tree accounting for several attenuation relationships, a larger number of seismic zones and parameters (e.g., b-values, activity rates, maximum magnitude) that refer to the earthquake catalog corrected for both statistical and historical completeness. In Figure 3 the UHSs corresponding to $T_R = 475$ yr calculated at 11 vibration periods for the two sites are shown. In the same figure the UHSs retrieved from the INGV Web site are also shown. The two benchmark UHSs correspond to the closest grid points to the S1 and S2 sites, for which INGV computed PSHA. Note that the UHSs are comparable, indicating general consistency between the hazard computed in the present study and that by INGV.

For the selected sites, the disaggregation analysis was also compared to that of INGV, which through the same Web site (see the Data and Resources section), provides disaggregation of seismic hazard in terms of contribution of M and R bins. In particular, a bin of 0.5 is used for M and a bin of 10 km is used for R. Concerning the ε variable, only the mean value from disaggregation is provided.

The comparison of disaggregated values in terms of modal and mean values for the two sites, obtained from the joint PDFs, is given in Table 2. In particular, $(\bar{M}, \bar{R}, \bar{\varepsilon})$ refer to the mean values, and $(M^*, R^*, \varepsilon^*)$ refer to the modal values (i.e., the maxima of the PDF). The results confirm also that, in terms of disaggregation, the present study and that of INGV are in general agreement. Table 3 lists the modal and mean values of the hazard variables for the two selected sites in the Sa($T = 1$ sec) case.

Figures 4 and 5 show the results of disaggregation for the S1 and S2 sites, respectively, obtained in the present study in terms of both joint and marginal PDFs. Because the joint PDF of equation (3) may be hardly represented in a figure, the three bivariate PDFs shown have been obtained by marginalizing each time on the third hazard variable not given in the plot. As an example, equation (7),

$$f(m, r|A > A_0) = \int_{\varepsilon} f(m, r, \varepsilon|A > A_0)\, d\varepsilon, \qquad (7)$$

indicates how to obtain the joint PDF of M and R only from that of M, R and ε. In each figure, left and right panels give the contributions in percents to PGA and Sa($T = 1$ sec) hazards, respectively. The central part of each panel shows specific joint PDFs for two of the three hazard variables. On the external axes, the marginal PDFs obtained from the joint PDFs are shown. The dashed black lines on the same axes refer to the results provided by INGV for PGA. As expected, disaggregation shows different results for the two sites. The joint and marginal PDFs for the site S1 have a unimodal shape for both PGA and Sa($T = 1$ sec). This is because the zone 927 (Fig. 1) where site S1 is located represents the most hazardous zone in terms of activity rate and maximum magnitude.

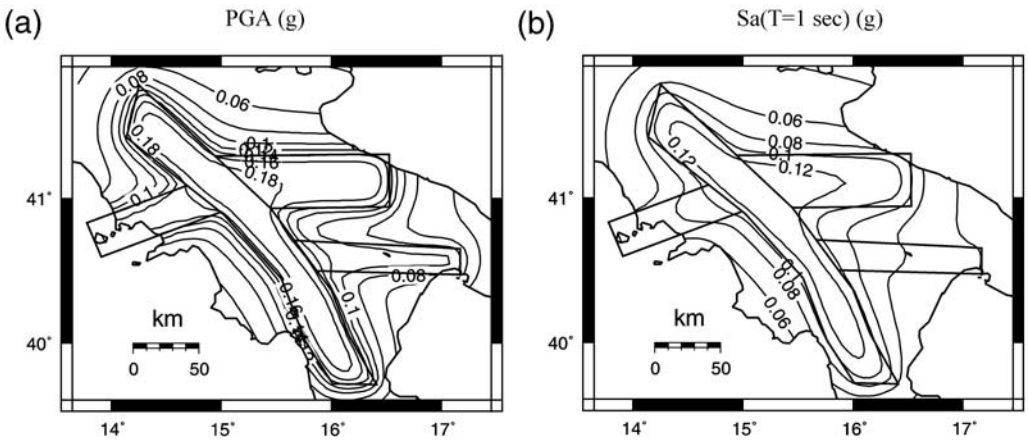

Figure 2. Hazard maps for PGA and Sa($T = 1$ sec) expressed in units of g for a 475 yr return period.

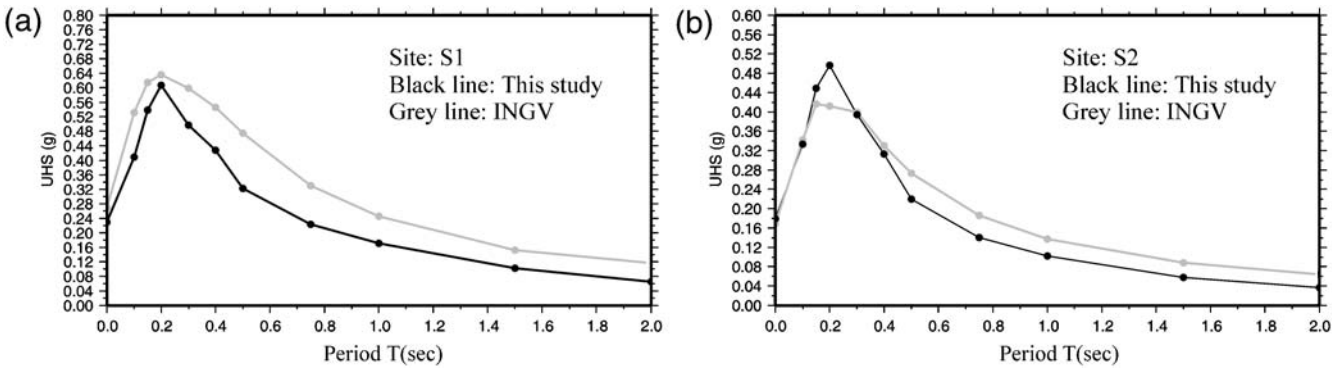

Figure 3. Uniform hazard spectra in g for (a) site S1 and for (b) site S2 for a 475 yr return period. Gray lines refer to the results provided by INGV and black lines refer to the results obtained in this study.

On the other hand, the PDFs for the site S2 are characterized by a bimodal shape for both PGA and Sa($T = 1$ sec). In fact, the disaggregated hazard level at site S2 is affected by both the zone 928 where the site is located and the nearest zone 927 (Fig. 1). This is confirmed by the presence of a most prominent mode, which corresponds to M 5.5 that is very close to the maximum magnitude value expected for zone 928 and a distance of 5.50 km. Although this first mode represents the greatest single contributor to the hazard, it may yet constitute a fraction of the total hazard from all other contributions. In fact, a second mode does exist and corresponds to magnitude and distance values that identify another design earthquake located in the zone 927 at a distance of 41.50 km having a M 7.0 that is very close to the maximum magnitude value expected for that zone. As an additional feature, a difference between PGA and Sa($T = 1$ sec) in the hazard contributions of the second mode can be noted. The larger contribution of high magnitude distant events observed in disaggregation of Sa($T = 1$ sec) hazard with respect to that of PGA can be ascribed to their lower

Table 2

Modal and Mean Values for the Hazard Variables for the Two Selected Sites S1 and S2 and for PGA*

	M^*	R^* (km)	ε^*	$\bar{M}$	$\bar{R}$ (km)	$\bar{\varepsilon}$
S1, Sant'Angelo dei Lombardi						
INGV	5.5–6.0	0.0–10.0	NA	6.06	8.44	0.76
This study	5.4	4.50	0.4	6.02	9.29	0.47
S2, Ponticelli						
INGV (first mode)	4.5–5.0	0.0–10.0	NA	5.05	9.91	1.00
Second mode	7.0–7.5	50.0–60.0	NA	—	—	—
This study (first mode)	5.5	5.50	0.4	5.21	6.09	0.67
Second mode	7.0	41.50	1.4	—	—	—

*The values have been retrieved from the joint PDFs. $\bar{M}$, and $\bar{R}$, $\bar{\varepsilon}$ refer to the mean values, and $\tilde{M}$, $\tilde{R}$, and $\tilde{\varepsilon}$ refer to the modal values.

Table 3

Modal and Mean Values of the Hazard Variables for the Two Selected Sites S1 and S2 and for Sa($T = 1$ sec)*

	M^*	R^* (km)	ε^*	$\tilde{M}$	$\bar{R}$ (km)	$\bar{\varepsilon}$
S1, Sant'Angelo dei Lombardi						
This study	6.2	8.5	0.4	6.34	16.11	0.504
S2, Ponticelli						
This study (first mode)	5.3	4.50	0.4	5.861	25.83	0.712
Second mode	7.0	66.50	0.4	-	-	-

*The values have been retrieved from the joint PDFs. $\bar{M}$, $\bar{R}$, and $\bar{\varepsilon}$ refer to the mean values, and $\tilde{M}$, $\tilde{R}$, and $\tilde{\varepsilon}$ refer to the modal values.

frequency content compared to lower magnitude nearby earthquakes affecting the spectral ordinates more at high frequency. As a consequence, for the selected spectral ordinate and return period, at least two design earthquakes do exist.

While the contribution of the second mode to PGA hazard (Fig. 5) may be eventually considered negligible, it is significant for Sa($T = 1$ sec) and of engineering interest. Although its contribution does not dominate disaggregation of Sa($T = 1$ sec) hazard, an engineer should prudently consider it in design as it may produce ground motion, having different characteristics with respect to the other design earthquake, which may affect the construction being designed.

These results have an important implication for this and other sites in the study region (as shown in the following). Because the fundamental period of most common engineering structures (i.e., buildings) is closer to 1 sec than 0 sec (corresponding to PGA), and a correlation exists between spectral ordinates at close periods (Inoue and Cornell, 1990), it may be not perfectly appropriate referring to disaggregation of PGA for the identification of the design earthquakes.

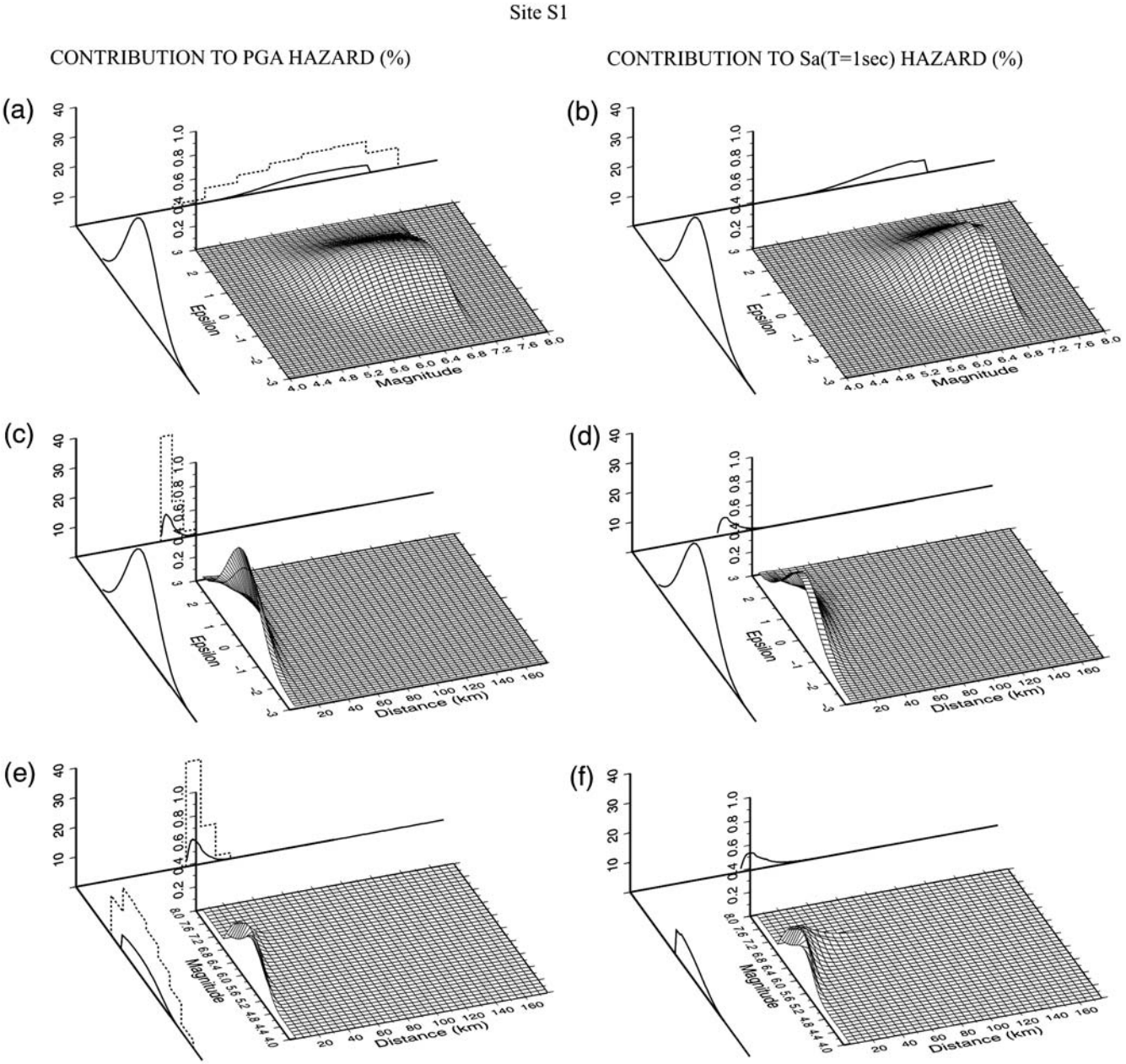

Figure 4. Disaggregation results expressed as contribution to 475 yr return period hazard for the site S1. Left panels refer to PGA and right panels refer to Sa($T = 1$ sec). The central part of each panel shows the joint PDFs for the specific hazard variable pair. On the external axes the marginal PDFs obtained from the joint PDFs area shown. The dashed black lines shown on the same axes refer to the results provided by INGV for PGA.

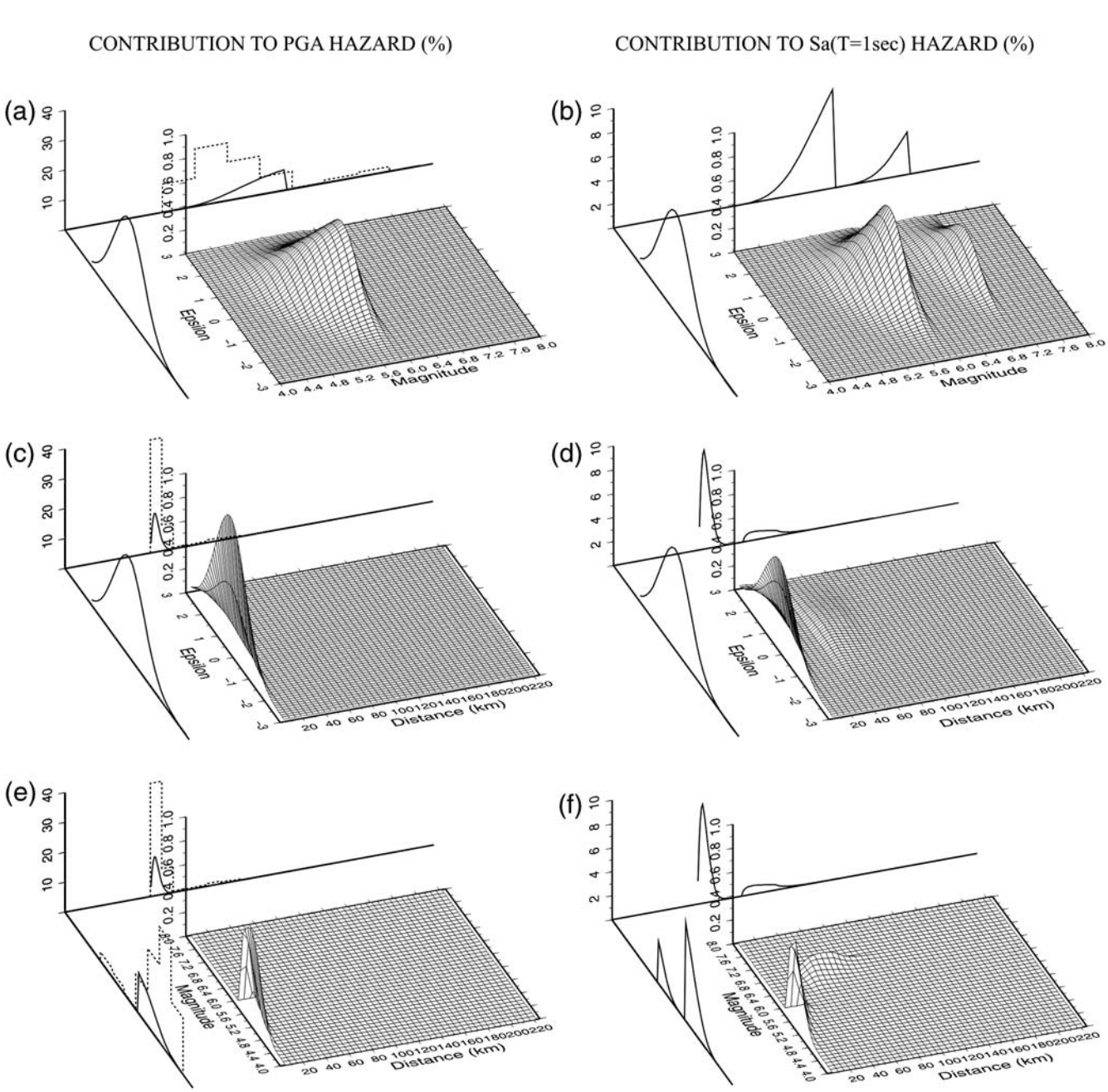

Figure 5. Same as Figure 4 but for site S2.

In fact, a sound definition of the design earthquakes is important because engineers who cannot afford to enter the hundreds or thousands of earthquake ground motions that are effectively considered in equation (2) into their analyses, at least need to consider the most relevant for the structural system for which the seismic assessment is carried out. The $M - R - \varepsilon$ maps in the following section help to define those major contributing earthquakes as a function of structural fundamental period, hazard level, and location in the southern Apennines.

Maps of Design Earthquakes

After computing the $T_R = 475$ years hazards for both PGA and Sa($T = 1$ sec), disaggregation was performed in terms of $M - R - \varepsilon$, and the modes of the PDFs were mapped for the area shown in Figure 1. These results, which may be interpreted as design earthquake maps, can be used as providers of additional information with respect to the standard hazard maps. Figure 6 shows the design earthquake maps in terms of magnitude, distance, and ε for PGA. In particular,

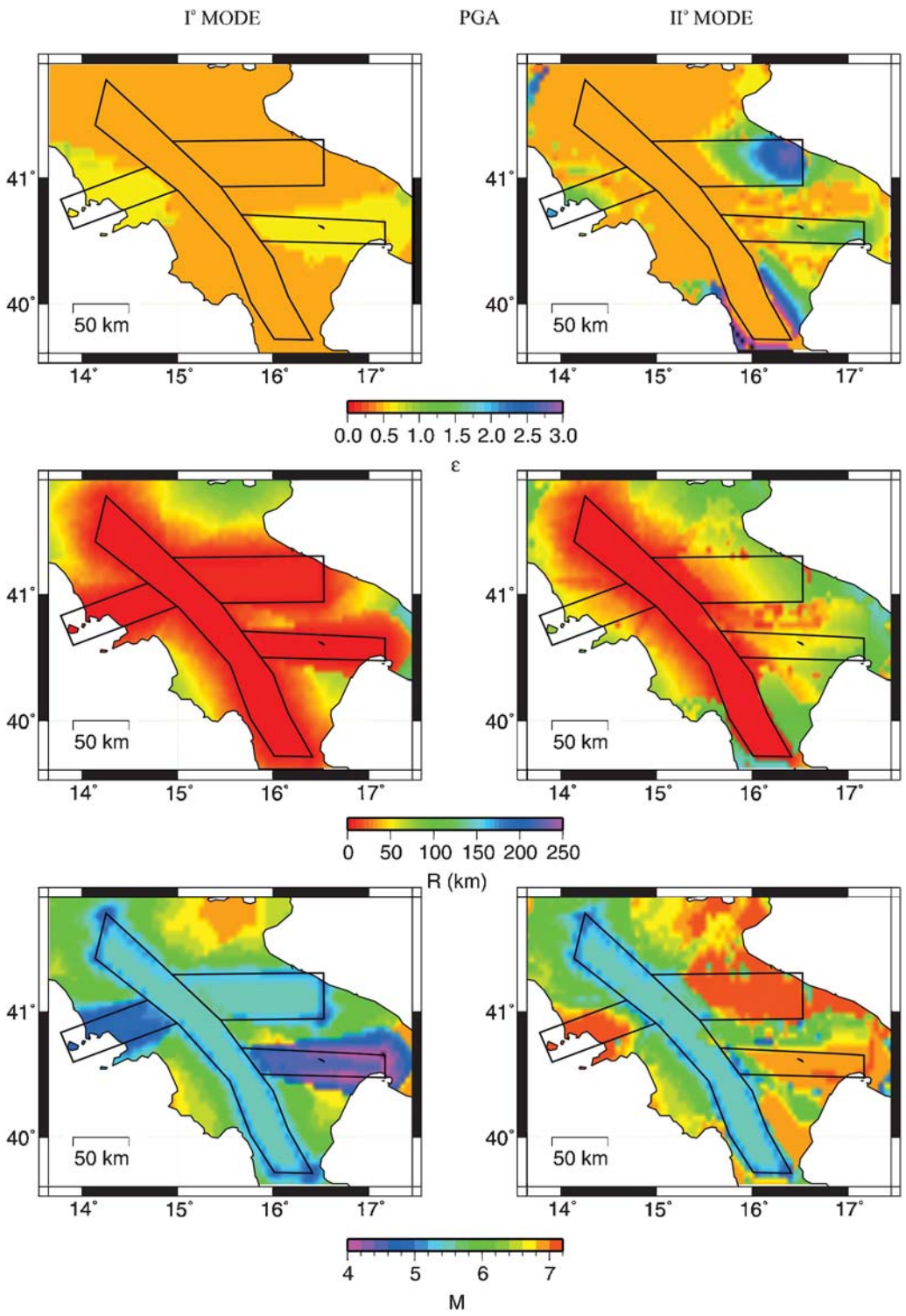

Figure 6. Design earthquakes maps for PGA for a return period of 475 yr. For each hazard variable, left panels refer to the first mode of the joint PDFs and right panels refer to the second mode of the joint PDFs.

left panels refer to the first mode of the joint PDF at each site, and right panels refer to the second mode, if any. The latter being identified if the differences between the relative maxima of the joint PDF were at least 0.25 in units of magnitude, 5.0 km in terms of distance, or 0.25 in terms of ε. Figure 7 shows the same results but for Sa($T = 1$ sec) indicating a strong connection, as expected, of the identified design earthquakes with the geometry of the seismic zones, the maximum magnitude values, and the selected activity rates (see Table 1).

A single design earthquake cannot be given for both PGA and Sa($T = 1$ sec) in a large portion of the study area. Larger magnitudes are required to explain target hazard values for Sa($T = 1$ sec) with respect to PGA. Except for the 926 and 928 seismic zones (Fig. 1) for the selected return period and particularly for PGA, the identification of hazard-dominant design earthquakes simply looking at the first mode requires the selection of earthquakes with magnitude around M 6.0 located at distances less than 10 km. Moreover, the magnitudes associated to the first mode correspond to values very close to the maximum magnitude expected for the seismic zones (Table 1). On the other hand, the second mode corresponds to larger magnitude values and larger distances, which accounts for the effect of other zones more hazardous with respect to that where the site is located.

Concerning the disaggregation in terms of distance, the results show a quite regular pattern. The distance associated with the design earthquakes increases as the distance of the site from the seismogenic areas increases. This affects both PGA and Sa($T = 1$ sec) in the 927 and 926 zones, where there is a difference of 3 in unit of magnitude values between first and second mode and at least a variation of 50 km in distance.

Disaggregation on the epsilon variable always shows positive values for all the zones with values ranging between 0.0 and 3.0, and in particular larger values are associated with second modes. This is consistent with the selected return period; in fact, larger ε values are associated to higher hazard levels.

To assess how the two modes compare, the contribution ratios of the modal values were calculated at each site for PGA and Sa($T = 1$ sec) hazards. This was carried out considering the two modes from the joint PDFs (Figs. 6 and 7) but also considering the first two modes identified on the marginal M, R, and ε PDFs separately. This also allows one to assess whether using marginal or joint PDFs from disaggregation leads to different conclusions on the design earthquakes in the study region. Figure 8 shows the results of the analysis for PGA (left panel) and Sa($T = 1$ sec) (right panel). The ΔF index corresponds to the relative contribution to the hazard ($\Delta F = F^{\mathrm{II}}/F^{\mathrm{I}}$) of the second mode ($F^{\mathrm{II}}$) with respect to the first mode (F^{I}). The white areas indicate sites where PDFs feature a single mode. Joint PDFs show larger areas where a second mode can be identified with respect to the marginal PDFs. For the areas external to the seismic zones, the second mode gives a comparable contribution to the hazard with respect to the first mode. This is because for those sites, multiple zones giving comparable contributions to the hazard exist.

The analysis of ΔF confirms what was observed for site S2 and shown in Figure 5, that is, the second mode gives a much higher contribution in the case of Sa($T = 1$ sec) with respect to PDFs. As expected, there is not a match between the results obtained from the joint and the marginal PGA for the whole study area.

Finally, it should be explained here how the presented results depend on the selected return period. For those sites where a close moderate earthquake and a distant large seismic event from another source zone dominate the hazard, the relative importance of the modes may be affected by the return period corresponding to the hazard level being disaggregated. In fact, although it may sound counterintuitive because of the attenuation features and site/sources relative location for return periods larger than 475 yr, the contribution to the hazard of the moderate and close events may increase with respect to the large and distant earthquakes representing the other mode.

Conclusions

The problem of selecting the design earthquake in southern Apennines, Italy, for earthquake engineering purposes was investigated using the probabilistic seismic hazard and disaggregation analyses. The design earthquakes for the area of interest were identified and mapped in order to illustrate the relationship with the geometry of the seismogenic zones and earthquake recurrence modeling parameters.

In the first stage of the study, the hazard analysis for PDFs and the spectral acceleration at $T = 1$ sec was performed. The acceleration values corresponding to a 475 yr return period were mapped. The application considered four seismic zones, which are the same of the national hazard study acknowledged by the Italian seismic code. Subsequently, the corresponding design earthquakes in terms of magnitude, distance, and ε were mapped. Site-specific analyses and disaggregation maps have shown that for a large part of the study area disaggregated joint and marginal PGA are characterized by at least a bimodal shape. The contribution to the hazard of the second modes is larger for Sa($T = 1$ sec) than for PGA and depends on the seismogenic zone.

The first modes for both spectral ordinates indicate that the magnitude of design earthquake has to be around M 6 for the central part of the southern Apennines. On the other hand, the zones 926 and 928 are characterized by magnitude around M 4.5 and 5.0, respectively. Magnitude values increase for all the seismogenic zones when the second modes are taken into account. The larger increase is in the zone 926 where the values change from M 4.5 for the first mode to M 7.0 for the second mode. The increase in the magnitude implies an increase of the distances at which the design earthquake has to be located. The analysis of the first mode shows that, for the sites located within the seismogenic areas, the largest contribution to the hazard comes from same zones. On the other hand, the analysis of the second modes shows that there is always a twofold contribution to the hazard that depends on the relative position of the site with respect to seismogenic areas.

Finally, maps of the relative contribution (ΔF) of the second mode with respect to the first mode of the disaggregated

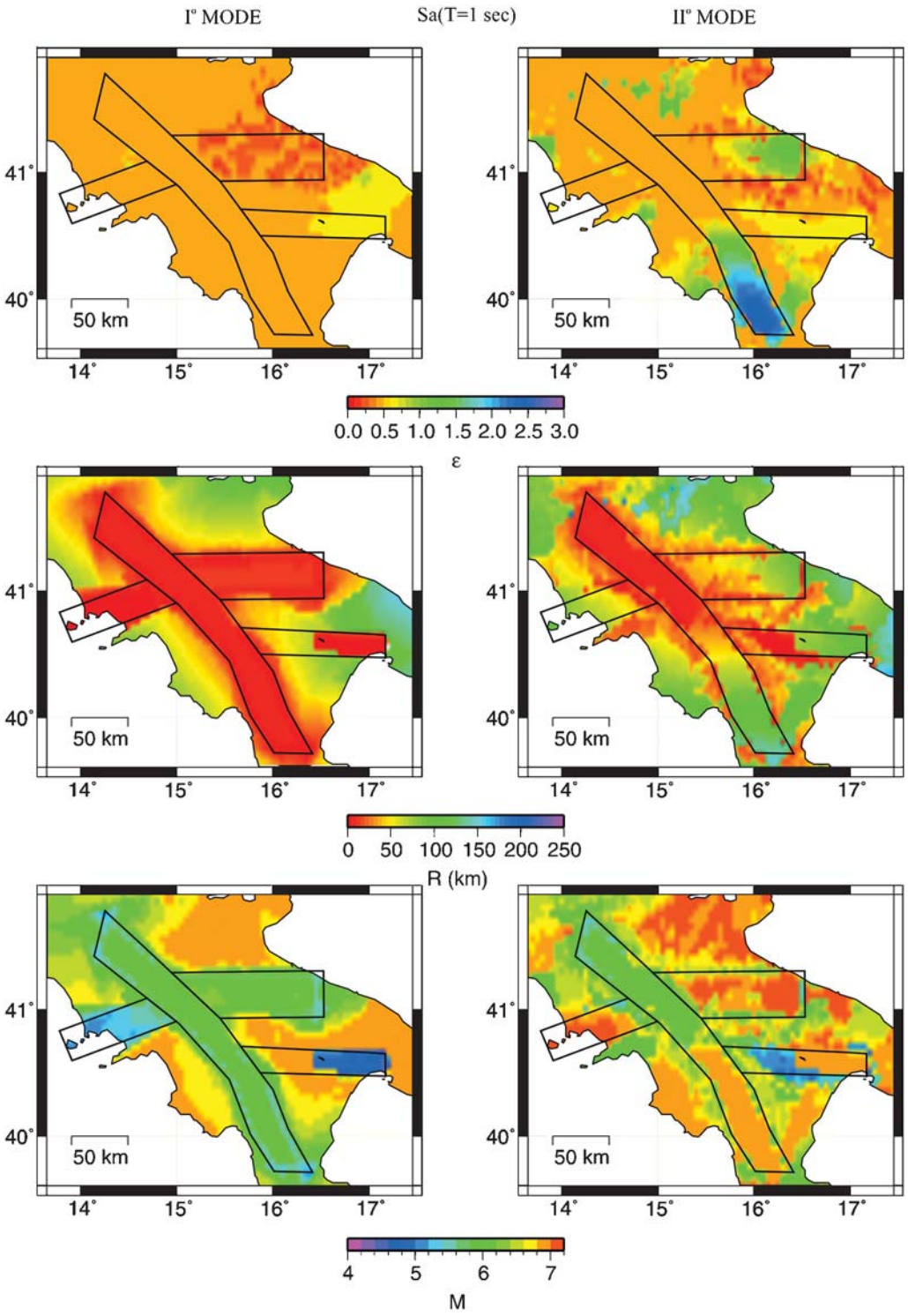

Figure 7. Same as Figure 6 but for Sa($T = 1$ sec).

marginal and joint PDFs were produced. As it is expected, the pattern of marginal PDFs is not matched by the pattern of the joint PDFs. In fact, the marginalization may lead to modal M, R pairs (i.e., the design earthquakes) different in number, values of the variables, and contribution to the hazard with respect to the joint PDF.

If disaggregation of Sa($T = 1$ sec) hazard is considered, the maps of ΔF show that the PDFs for many sites feature a bimodal shape indicating multiple design earthquakes, which may be significant for engineering purposes. Conversely, disaggregation of PGA hazard is typically unimodal or characterized by a second mode modestly contributing to the hazard

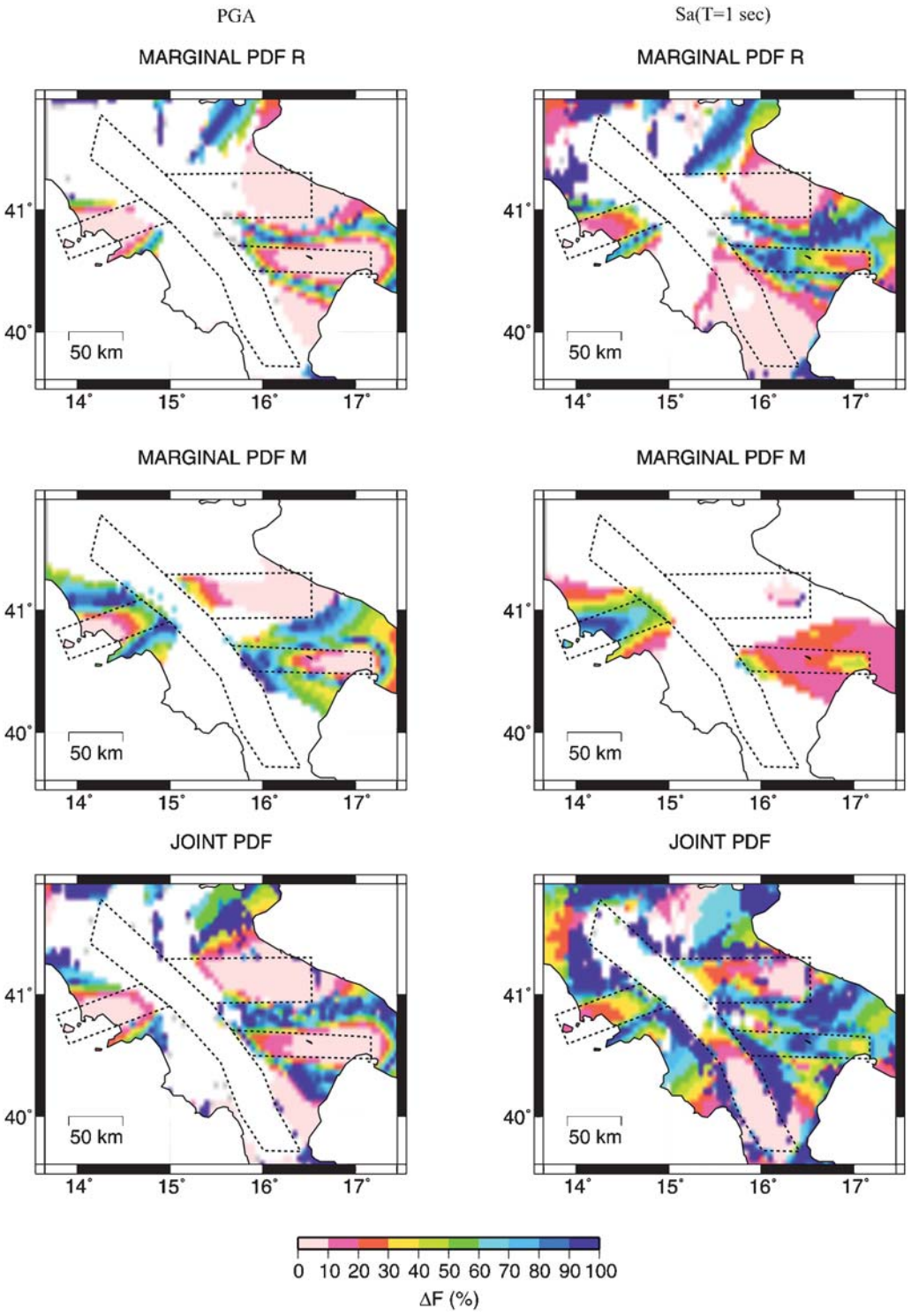

Figure 8. Maps of the relative contribution (ΔF) of the second mode with respect to the first mode of the PDFs obtained from disaggregation analysis. Left panels refer to PGA and right panels refer to Sa($T = 1$ sec).

with respect to the first mode, which could lead a practitioner to consider only the latter and to imprudently neglect the former.

In conclusion, mapping the design earthquakes may prove useful and can be used as additional information with respect to the classic hazard maps. It, in the case of engineering risk assessment, allows the practitioner to account for the effect of multiple events and ground-motion parameters in those region, as the one the study refers to, where PSHA is based on seismogenic zones.

Data and Resources

Hazard data from INGV were retrieved via the Progetto S1 Web site: http://esse1-gis.mi.ingv.it/s1_en.php (last accessed September 2008). The CPTI04 catalog can be accessed at http://emidius.mi.ingv.it/CPTI04 (last accessed January 2009).

Acknowledgments

This work was supported by the Italian Dipartimento della Protezione Civile as part of the 2005–2008 ReLUIS project and partially by the project S3 in the framework of the 2007–2009 DPC-INGV agreement. The authors greatly appreciate discussion and revisions from the *BSSA* associate editor Ivan Wong and the two anonymous reviewers, as they significantly improved quality and readability of the paper. Finally, we are grateful to R. K. Hagen of Stanford University who proofread the paper. The figures were prepared with Generic Mapping Tools (Wessel and Smith, 1991).

References

Baker, J. W., and C. A. Cornell (2006). Spectral shape, epsilon and record selection, *Earthq. Eng. Struct. Dyn.* **35,** no. 9, 1077–1095.

Bazzurro, P., and C. A. Cornell (1999). Disaggregation of seismic hazard, *Bull. Seismol. Soc. Am.* **89,** 501–520.

Benjamin, J. R., and C. A. Cornell (1970). *Probability, Statistics, and Decision for Civil Engineers*, McGraw-Hill, New York.

Bommer, J. J. (2004). Earthquake actions in seismic codes: Can current approaches meet the needs of PBSD? in *Performance Based Seismic Design Concepts and Implementation*, PEER Rept. 2004/05, Pacific Earthquake Engineering Research Center, University of California, Berkeley.

Cinti, F. R., L. Faenza, W. Marzocchi, and P. Montone (2004). Probability map of the next $M \geq 5.5$ earthquakes in Italy, *Geochem. Geophys. Geosyst.* **5,** Q1103.

Convertito, V., and A. Herrero (2004). Influence of focal mechanism in probabilistic seismic hazard analysis, *Bull. Seismol. Soc. Am.* **94,** 2124–2136.

Cornell, C. A. (1968). Engineering seismic risk analysis, *Bull. Seismol. Soc. Am.* **58,** 1583–1606.

Cornell, C. A. (2004). Hazard, ground motions and probabilistic assessment for PBSD, in *Performance Based Seismic Design Concepts and Implementation*. PEER Rept. 2004/05, Pacific Earthquake Engineering Research Center, University of California, Berkeley.

Cornell, C. A. (2005). On earthquake record selection for nonlinear dynamic analysis, *The Esteva Symposium*, Mexico, August 2005 (http://www.stanford.edu/group/rms/RMS_Papers/pdf/Allin/).

Cramer, H. C., and M. D. Petersen (1996). Predominant seismic source distance and magnitude for Los Angeles, Orange, and Ventura Counties, California, *Bull. Seismol. Soc. Am.* **86,** 1645–1649.

CS.LL.PP. (2008). DM 14 gennaio 2008 Norme Tecniche per le Costruzioni, *Gazzetta Ufficiale della Repubblica Italiana* **29** (in Italian).

Di Sarno, L., E. Cosenza, B. De Risi, and C. Mascolo (2006). Application of base isolation to a new building of Naples, *Proc. of the World Conference on Structural Control*, San Diego, Paper no. 173 (CD-ROM).

EN 1998-1 (2004). Eurocode 8: Design of structures for earthquake resistance, Part 1: General rules, seismic actions and rules for buildings, European Committee for Standardization (CEN), Brussels.

Gruppo di lavoro Catalogo Parametrico dei Terremoti Italiani (CPTI) (2004). Catalogo Parametrico dei Terremoti Italiani, versione 2004 (CPTI04), INGV, Bologna.

Gutenberg, B., and C. R. Richter (1944). Frequency of earthquakes in California, *Bull. Seismol. Soc. Am.* **34,** 185–188.

Harmsen, S., and A. Frankel (2001). Geographic deaggregation of seismic hazard in the United States, *Bull. Seismol. Soc. Am.* **91,** 13–26.

Iervolino, I., and C. A. Cornell (2005). Record selection for nonlinear seismic analysis of structures, *Earthq. Spectra* **21,** 685–713.

Iervolino, I., and C. A. Cornell (2008). Probability of occurrence of velocity pulses in near-source ground motions, *Bull. Seismol. Soc. Am.* **98,** 2262–2277.

Iervolino, I., G. Maddaloni, and E. Cosenza (2008). Eurocode 8 compliant real record sets for seismic analysis of structures, *J. Earthq. Eng.* **12,** no. 1, 54–90.

Iervolino, I., G. Maddaloni, and E. Cosenza (2009). A note on selection of time-histories for seismic analysis of bridges in Eurocode 8, *J. Earthq. Eng.* (in press)

Inoue, T., and C. A. Cornell (1990). Seismic hazard analysis of multi-degree-of-freedom structures, *Reliability of Marine Structures (RMS)-8*, Stanford, California, 70 pp.

McGuire, R. K. (1995). Probabilistic seismic hazard analysis and design earthquakes: Closing the loop, *Bull. Seismol. Soc. Am.* **85,** 1275–1284.

Meletti, C., and V. Montaldo (2007). Stime di pericolosità sismica per diverse probabilità di superamento in 50 anni: Valori di a_g, *Progetto DPC-INGV S1, Deliverable D2* (http://esse1.mi.ingv.it/d2.html) (in Italian).

Meletti, C., F. Galadini, G. Valensise, M. Stucchi, R. Basili, S. Barba, G. Vannucci, and E. Boschi (2008). A seismic source zone model for the seismic hazard assessment of the Italian territory, *Tectonophysics* **450,** 85–108.

Montaldo, V., and C. Meletti (2007). Valutazione del valore della ordinata spettrale a 1 sec e ad altri periodi di interesse ingegneristico, *Progetto DPC-INGV S1, Deliverable D3* (http://esse1.mi.ingv.it/d3.html) (in Italian).

Montone, P., M. T. Mariucci, S. Pondrelli, and A. Amato (2004). An improved stress map for Italy and surrounding regions (Central Mediterranean), *J. Geophys. Res.* **109,** B10410, doi 10.1029/2003JB002703.

Reiter, L. (1990). *Earthquake Hazard Analysis*, Columbia University Press, New York, 254 pp.

Sabetta, F., and A. Pugliese (1996). Estimation of response spectra and simulation of non stationary earthquake ground motion, *Bull. Seismol. Soc. Am.* **86,** 337–352.

Spallarossa, D., and S. Barani (2007). Disaggregazione della pericolosità sismica in termini di $M - R - \varepsilon$, *Progetto DPC-INGV S1, Deliverable D14* (http://esse1.mi.ingv.it/d14.html) (in Italian).

U.S. Nuclear Regulatory Commission (2001). Technical basis for revision of regulatory guidance on design ground motions: Hazard- and risk-consistent ground motion spectra guidelines, NUREG/CR-6728, Government Printing Office, Washington, D.C.

Valensise, G., A. Amato, P. Montone, and D. Pantosti (2003). Earthquakes in Italy: Past, present and future, *Episodes* **26,** 245–249.

Wessel, P., and W. H. F. Smith (1991). Free software helps map and display data, *Eos Trans. Am. Geophys. Union* **72,** 445–446.

Westaway, R., and J. Jackson (1987). The earthquake of 1980 November 23 in Campania–Basilicata (southern Italy), *Geophys. J. R. Astron. Soc.* **90,** 375–443.

Istituto Nazionale di Geofisica e Vulcanologia
Osservatorio Vesuviano
Via Diocleziano 328
80124 Napoli, Italy
(V.C.)

Dipartimento di Ingegneria Strutturale
Università degli studi di Napoli Federico II
Via Claudio 21
80125, Napoli, Italy
(I.I.)

Istituto Nazionale di Geofisica e Vulcanologia
Via di Vigna Murata, 605
00143 Roma, Italy
(A.H.)

Manuscript received 18 September 2008